3888 *Inorg. Chem.* **2010**, *49*, 3888–3895
DOI: 10.1021/ic1000478

Inorganic Chemistry
Article

# Intercalation of Ethylene Glycol into Yttrium Hydroxide Layered Materials

**Yuanzhou Xi and Robert J. Davis***

*Department of Chemical Engineering, University of Virginia, 102 Engineers' Way, P.O. Box 400741, Charlottesville, Virginia 22904-4741*

Received January 8, 2010

Intercalation of ethylene glycol into layered yttrium hydroxide containing nitrate counterions was accomplished by heating the reagents in a methanol solution of sodium methoxide under autogenous pressure at 413 K for 20 h. The resulting crystalline material had an expanded interlayer distance of 10.96 Å, confirming the intercalation of an ethylene glycol derived species. Characterization of the material by FT-IR spectroscopy, thermogravimetric analysis, and the catalytic transesterification of tributyrin with methanol was consistent with direct bonding of ethylene glycolate anions ($O_2C_2H_5^-$) to the yttrium hydroxide layers, forming Y−O−C bonds. The layers of the material are proposed to be held together by H-bonding between the hydroxyls of grafted ethylene glycol molecules attached to adjacent layers. Glycerol can also be intercalated into yttrium hydroxide layered materials by a similar method.

## 1. Introduction

The layered double hydroxide (LDH) materials and their derived materials have attracted intensive research interest because of their potential applications as heterogeneous catalysts,[1−5] adsorbents[6,7] and drug delivery vehicles.[8,9] The layered double hydroxide known as hydrotalcite, with a general formula of $[M^{2+}_{(1-x)}M^{3+}_{x}(OH)_2]^{x+}A^{m-}_{x/m}\cdot nH_2O$, represents one of the most commonly studied anionic clays. Hydrotalcites are composed of brucite-like layers with charge balancing anions and water molecules residing in the interlayer regions. The brucite-like layer contains di- and trivalent cations octahedrally coordinated by hydroxyl groups. The anion exchange properties and intercalation compounds of LDHs have been explored previously.[8,10−15]

A new type of pillared crystalline compound of $[R_4(OH)_{10}(H_2O)_4]_nA_n$ (R = rare-earth ions, A = intercalated organic anions, 2,6-naphthalenedisulfonate ($NDS^{2-}$), and 2,6-anthraquinonedisulfonate ($AQDS^{2-}$)) was reported recently by Gandara et al.[16] A representative layered structure of this type material is displayed in Scheme 1. The positively charged layers of the new rare-earth hydroxides are composed of trivalent rare-earth hydroxocations. For example, the layers of $[R_4(OH)_{10}(H_2O)_4]^{2+}_n$ are composed of eight- and nine-coordinated rare-earth cations, linked by $\mu_3$-hydroxyls and one water molecule to form two different polyhedra: a dodecahedron and a monocapped square antiprism.[16] The layered rare-earth hydroxide materials are expected to exhibit not only anion exchange properties but could also have interesting catalytic activity and rich intercalation chemistry.[16] Indeed, the layered rare-earth hydroxide $[Yb_4(OH)_{10}(H_2O)_4]$[2,6-AQDS] was active and selective in the catalytic oxidation of methylphenylsulfide by $H_2O_2$.[17] The preparation, crystal structure determination, and anion exchange

*To whom correspondence should be addressed. E-mail: rjd4f@virginia.edu. Phone: 434-924-6284. Fax: 434-982-2658.

(1) Cavani, F.; Trifiro, F.; Vaccari, A. *Catal. Today* **1991**, *11*, 173.
(2) Sels, B. F.; De Vos, D. E.; Jacobs, P. A. *Catal. Rev.* **2001**, *43*, 443.
(3) Climent, M. J.; Corma, A.; Iborra, S.; Velty, A. *J. Catal.* **2004**, *221*, 474.
(4) Roeffaers, M. B. J.; Sels, B. F.; Uji-i, H.; De Schryver, F. C.; Jacobs, P. A.; De Vos, D. E.; Hofkens, J. *Nature* **2006**, *439*, 572.
(5) Pinnavaia, T. J. *Science* **1983**, *220*, 365.
(6) Pavan, P. C.; Gomes, G. D.; Valim, J. B. *Micropor. Mesopor. Mater.* **1998**, *21*, 659.
(7) You, Y. W.; Zhao, H. T.; Vance, G. F. *Appl. Clay Sci.* **2002**, *21*, 217.
(8) Wei, M.; Pu, M.; Guo, J.; Han, J. B.; Li, F.; He, J.; Evans, D. G.; Duan, X. *Chem. Mater.* **2008**, *20*, 5169.
(9) Kwak, S. Y.; Kriven, W. M.; Wallig, M. A.; Choy, J. H. *Biomaterials* **2004**, *25*, 5995.
(10) Miyata, S. *Clays Clay Miner.* **1983**, *31*, 305.
(11) Meyn, M.; Beneke, K.; Lagaly, G. *Inorg. Chem.* **1990**, *29*, 5201.
(12) Liu, Z. P.; Ma, R. Z.; Osada, M.; Iyi, N.; Ebina, Y.; Takada, K.; Sasaki, T. *J. Am. Chem. Soc.* **2006**, *128*, 4872.
(13) Thyveetil, M. A.; Coveney, P. V.; Greenwell, H. C.; Suter, J. L. *J. Am. Chem. Soc.* **2008**, *130*, 4742.
(14) Aguzzi, A.; Ambrogi, V.; Costantino, U.; Marmottini, F. *J. Phys. Chem. Solids* **2007**, *68*, 808.
(15) Guimaraes, J. L.; Marangoni, R.; Ramos, L. P.; Wypych, F. *J. Colloid Interface Sci.* **2000**, *227*, 445.
(16) Gandara, F.; Perles, J.; Snejko, N.; Iglesias, M.; Gomez-Lor, B.; Gutierrez-Puebla, E.; Monge, M. A. *Angew. Chem., Int. Ed.* **2006**, *45*, 7998.
(17) Gandara, F.; Puebla, E. G.; Iglesias, M.; Proserpio, D. M.; Snejko, N.; Monge, M. A. *Chem. Mater.* **2009**, *21*, 655.
(18) McIntyre, L. J.; Jackson, L. K.; Fogg, A. M. *Chem. Mater.* **2008**, *20*, 335.
(19) McIntyre, L. J.; Jackson, L. K.; Fogg, A. M. *J. Phys. Chem. Solids* **2008**, *69*, 1070.
(20) Poudret, L.; Prior, T. J.; McIntyre, L. J.; Fogg, A. M. *Chem. Mater.* **2008**, *20*, 7447.
(21) Geng, F.; Hin, H.; Matsushita, Y.; Ma, R.; Tanaka, M.; Iyi, N.; Sasaki, T. *Chem.—Eur. J.* **2008**, *14*, 9255.
(22) Geng, F. X.; Matsushita, Y.; Mat, R. Z.; Xin, H.; Tanaka, M.; Izumi, F.; Iyi, N.; Sasaki, T. *J. Am. Chem. Soc.* **2008**, *130*, 16344.

 Published on Web 03/19/2010 

**Scheme 1.** Model Structure of Rare-Earth Hydroxide Layered Material[a]

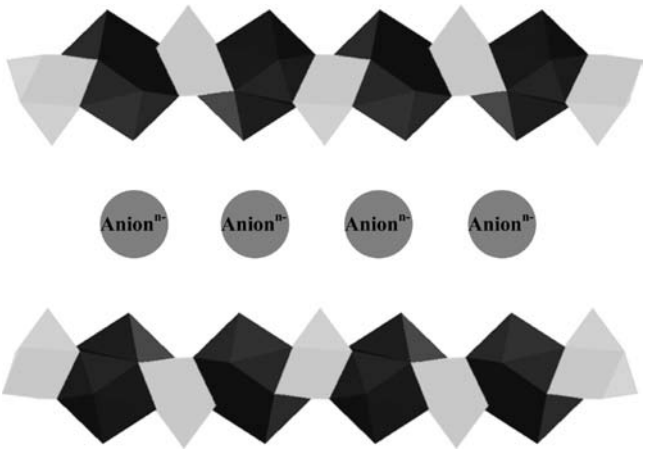


[a] Derived from the Cambridge Crystallographic Data Centre (CCDC-604276) at http://www.ccdc.cam.ac.uk/data_request/cif.

properties of various layered lanthanide/rare-earth hydroxide materials were also reported recently.[18−24]

The layered rare-earth hydroxide materials readily exchange anions located in the interlayer regions. For example, McIntyre et al. reported that $Ln_2(OH)_5(NO_3)\cdot xH_2O$ (Ln = Y, Gd−Lu) can completely exchange the interlayer nitrate anions with a range of organic carboxylate and sulfonate anions at room temperature.[18,19] Layered hydroxide materials with composition of $Ln_2(OH)_5X\cdot 1.5H_2O$ (X = Cl, Br; Ln = Y, Dy, Er, Yb) readily exchange the halide anions with a number of organic dicarboxylates at room temperature.[20] Geng et al. also observed that the interlayer $Cl^-$ of $RE(OH)_{2.5}Cl_{0.5}\cdot 0.8H_2O$ (RE = Eu, Tb, etc.) can be readily exchanged by a variety of anions ($NO_3^-$, $SO_4^{2-}$, dodecylsulfonate, etc.) at room temperature.[21]

Layered materials are promising precursors in the synthesis of inorganic−organic compounds. Many researchers reported intercalation of ethylene glycol and/or glycerol into various layered materials such as kaolinite,[25,26] brucite,[27] Zn−Al−$CO_3$ LDH,[15] Mg−Al−$CO_3$ hydrotalcite,[28] boehmite,[29,30] layered compound of FeOCl[31] and layered basic zinc acetate.[32] Both neutral ethylene glycol and grafted ethylene glycol by forming M−O−C (M: metal) bonds were reported to exist depending on the type of host layer and the method of intercalation. The inorganic−organic compounds derived from layered materials have potential applications in catalysts, polymer fillers, absorbents, chromatographic materials, and pigments.[25−27,30]

In the current work, we report on the intercalation of ethylene glycol and glycerol into yttrium hydroxynitrate layered materials. The resulting materials were evaluated as catalysts for the transesterification of tributyrin, a model reaction for the synthesis of biodiesel fuel from triglycerides.

## 2. Experimental Methods

**2.1. Material Synthesis.** The $Y_2(OH)_5NO_3\cdot xH_2O$ was synthesized according to the procedures reported by McIntyre et al.[18,19] A 375 mL aqueous solution containing 63.20 g of $Y(NO_3)_3\cdot 6H_2O$ (Sigma-Aldrich, 99.9%) was added to a 125 mL aqueous solution containing 10.50 g of NaOH (Mallinckrodt, 98.6%) and 15.30 g of $NaNO_3$ (Fluka, 99.8%). The mixture was sealed into Teflon vessels and held in an oven at 398 K for 48 h. The resulting solid was then separated by centrifugation and washed thoroughly with distilled deionized (DDI) water. The solid material was dried in an oven at 338 K overnight and then ground into powder and sieved between 0.038 and 0.075 mm. The resulting white material was denoted as YHN.

The anion exchange of terephthalic acid anion with YHN was conducted by adding 0.5 g of YHN into 50 mL of aqueous solution of 0.11 M terephthalic acid disodium salt (Sigma-Aldrich, 96%) and stirring at 800 rpm at room temperature for 100 min. The resulting solid was then separated by centrifugation and washed with 200 mL of anhydrous methanol (Sigma-Aldrich, 99.8%) and dried under flowing $N_2$ (100 $cm^3$ $min^{-1}$, Messer, 99.999%) overnight at room temperature. The obtained solid was denoted as YHN-TA.

The intercalation of ethylene glycol into YHN was performed with the following procedure: 0.5 g of YHN and 0.05 mol ethylene glycol (99.8%, Sigma-Aldrich) were added into 100 mL of 0.5 M sodium methoxide/methanol solution (Sigma-Aldrich). The mixture was sealed into a Teflon vessel and heated in an oven at 413 K for 20 h. The resulting solid was then separated, washed, and dried with the same method used for YHN-TA. The obtained solid was denoted as YHN-NaM-EG. When the sample was used for transesterification, YHN-NaM-EG was recovered immediately after washing with methanol and charged into the reactor.

The intercalation of glycerol was accomplished by sealing 0.5 g of YHN, 0.05 mol of glycerol (99.6%, Acros), and 100 mL of 0.5 M sodium methoxide/methanol solution (Sigma-Aldrich) into a Teflon vessel and treated with the same conditions described above for the preparation of YHN-NaM-EG. The glycerol intercalated sample is denoted by YHN-NaM-GL.

For comparison purposes, YHN-M (by mixing 0.5 g of YHN and 100 mL of methanol), YHN-M-EG (by mixing 0.5 g of YHN, 100 mL of methanol and 0.05 mol of ethylene glycol) and YHN-NaM (by mixing 0.5 g of YHN and 100 mL of 0.5 M sodium methoxide/methanol solution) were also prepared with the same conditions as for preparing YHN-NaM-EG, except for the mixture compositions. These samples were used to explore the role of methoxide on the intercalation chemistry of ethylene glycol.

**2.2. Material Characterization.** Thermogravimetric analysis (TGA) was performed on a TGA 2050 Thermogravimetric Analyzer (TA Instruments). Approximately 40 mg of YHN sample or its derived material was loaded into the instrument, and the temperature was ramped from room temperature to 1073 at 2 K $min^{-1}$ under 100 $cm^3$ $min^{-1}$ of flowing air. X-ray diffraction (XRD) was obtained on a Scintag XDS 2000 diffractometer using Cu Kα radiation ($\lambda$ = 1.54 Å). Samples were scanned continuously from 4° to 72° at a scan rate of 2° $min^{-1}$. Scanning electron microscopy (SEM) was performed on a JEOL-6700F field emission microscope. Samples were coated with Au/Pd prior to imaging. The Fourier transformed infrared spectra were obtained with a BIO-RAD FTS-60A spectrometer equipped with a liquid $N_2$-cooled MCT detector. Liquid samples were studied in the transmission mode. Solid samples were diluted in KBr powder to 5 wt %, and spectra were recorded in

(23) Geng, F. X.; Matsushita, Y.; Ma, R. Z.; Xin, H.; Tanaka, M.; Iyi, N.; Sasaki, T. *Inorg. Chem.* **2009**, *48*, 6724.
(24) Lee, K. H.; Byeon, S. H. *Eur. J. Inorg. Chem.* **2009**, 929.
(25) Tunney, J. J.; Detellier, C. *Clays Clay Miner.* **1994**, *42*, 552.
(26) Janek, M.; Emmerich, K.; Heissler, S.; Nuesch, R. *Chem. Mater.* **2007**, *19*, 684.
(27) Wypych, F.; Schreiner, W. H.; Marangoni, R. *J. Colloid Interface Sci.* **2002**, *253*, 180.
(28) Stanimirova, T.; Hibino, T. *Appl. Clay Sci.* **2006**, *31*, 65.
(29) Inoue, M.; Kondo, Y.; Inui, T. *Inorg. Chem.* **1988**, *27*, 215.
(30) Inoue, M.; Kominami, H.; Kondo, Y.; Inui, T. *Chem. Mater.* **1997**, *9*, 1614.
(31) Kikkawa, S.; Kanamaru, F.; Koizumi, M. *Inorg. Chem.* **1980**, *19*, 259.
(32) Kasai, A.; Fujihara, S. *Inorg. Chem.* **2006**, *45*, 415.

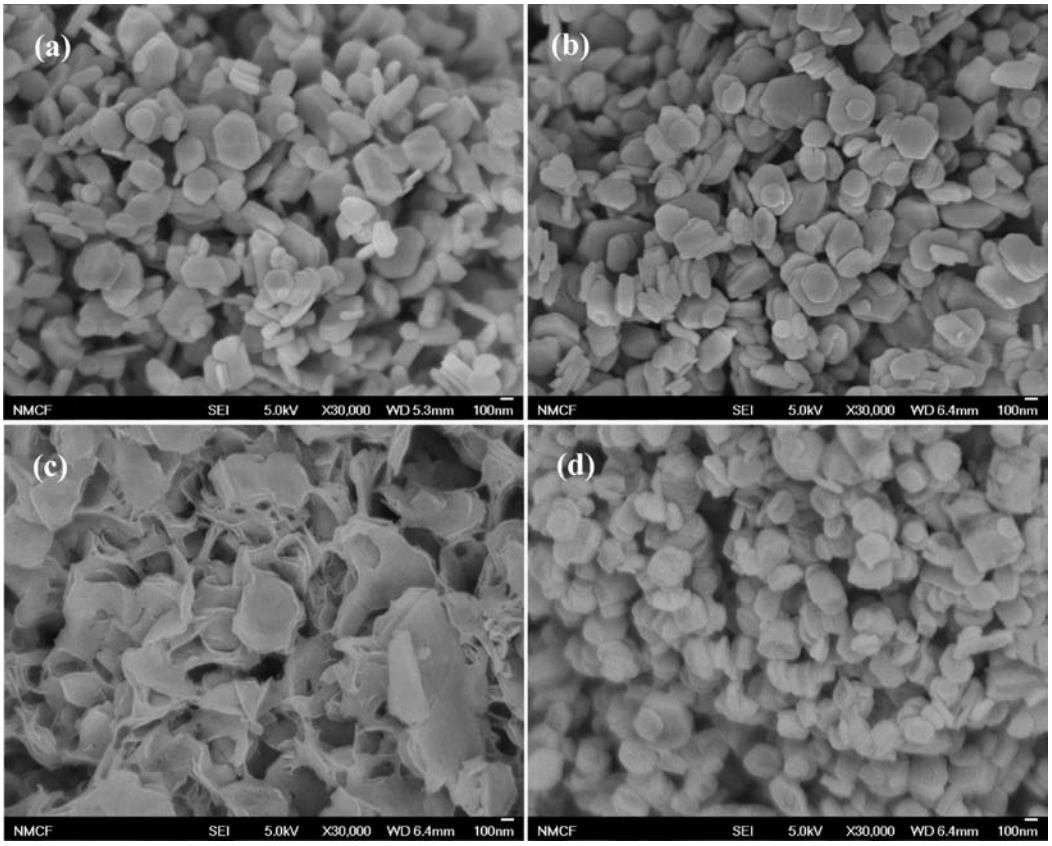


**Figure 1.** Scanning electron micrographs of (a) YHN; (b) YHN-M; (c) YHN-NaM; (d) YHN-NaM-EG.

the diffuse reflectance mode by using a Harrick Praying Mantis diffuse reflectance accessory. All spectra were averaged by accumulating 100 scans at a resolution of 4 $cm^{-1}$ in the range of 400−4000 $cm^{-1}$. The Brunauer−Emmett−Teller (BET) surface area was measured by $N_2$ adsorption at 77 K using a Micromeritics ASAP 2020 adsorption system. Samples were degassed for 2 h at room temperature before conducting $N_2$ adsorption experiments. The content of yttrium and sodium was measured by ICP analysis (Galbraith Laboratories, Knoxville, TN), and carbon was measured with a PerkinElmer 240 Elemental Analyzer (Galbraith Laboratories, Knoxville, TN).

**2.3. Transesterification.** Transesterification of tributyrin with methanol was used as a probe reaction for the YHN-NaM-EG sample. The reaction was conducted in a 250 mL 3-neck round-bottom flask at 333 K in an oil bath and magnetically stirred at 800 rpm. The reactor was equipped with a reflux condenser and was continuously purged with flowing $N_2$ at 40 $cm^3$ $min^{-1}$. In each run, 68.25 g of methanol and 21.9 g of purified tributyrin[33] were charged into the reactor with 3.3 g of dibutyl ether (Aldrich, 99.3%) as an internal standard. After the temperature of the reactants reached 333 K, the YHN-NaM-EG prepared from 0.5 g of YHN was charged into the reactor to initiate the reaction. Liquid samples were removed from the reactor at different time intervals and analyzed for products using the same procedure described in our previous work.[34] After the reaction was conducted for about 17 h, the used catalyst was separated from the liquid products by centrifugation and charged back into the reactor with fresh reactants. After the second reaction was conducted for about 23 h, the used catalyst was removed by centrifugation, washed with 200 mL of methanol, and dried under flowing dry $N_2$ (100 $cm^3$ $min^{-1}$) at room temperature prior to characterization.

The transesterification of tributyrin (T) with methanol (M) proceeds in three consecutive steps as shown below with methyl butyrate (MB) and glycerol (G) as final products and dibutyrin (D) and monobutyrin (Mo) as intermediate products.[33−35]

$$T + M \rightarrow D + MB \quad (1)$$

$$D + M \rightarrow Mo + MB \quad (2)$$

$$Mo + M \rightarrow G + MB \quad (3)$$

## 3. Results and Discussion

**3.1. SEM.** The morphology of hydrothermally synthesized yttrium hydroxynitrate (YHN) and its derived materials, YHN-M, YHN-NaM, and YHN-NaM-EG, were visualized by SEM as shown in Figure 1. The YHN sample was composed of crystalline powders with hexagonal platelet morphology as shown in Figure 1a, consistent with previously reported results.[18,19] The YHN sample had a platelet size of about 300 nm in the long direction with approximate 50 nm platelet thickness. The methanol-treated sample, YHN-M, (Figure 1b) and the sample treated with ethylene glycol and sodium methoxide YHN-NaM-EG (Figure 1d) have a similar morphology to YHN except the latter sample had a slightly greater platelet thickness than the YHN sample. In contrast to the regular crystalline platelets observed in the

(33) Xi, Y.; Davis, R. J. *J. Catal.* **2009**, *268*, 307.
(34) Xi, Y.; Davis, R. J. *J. Catal.* **2008**, *254*, 190.
(35) Cantrell, D. G.; Gillie, L. J.; Lee, A. F.; Wilson, K. *Appl. Catal., A* **2005**, *287*, 183.

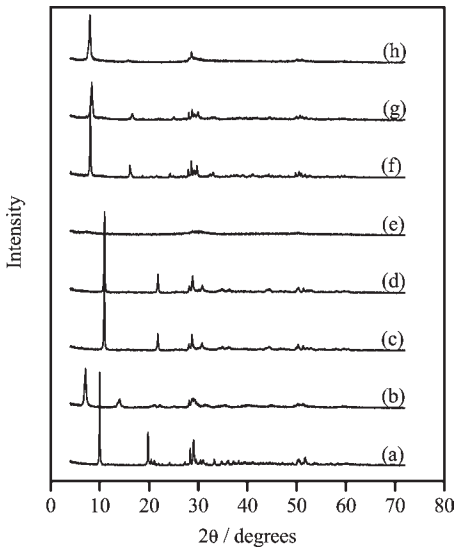


**Figure 2.** XRD spectra of (a) YHN; (b) YHN-TA; (c) YHN-M; (d) YHN-M-EG; (e) YHN-NaM; (f) YHN-NaM-EG; (g) YHN-NaM-EG after 2 transesterification reaction cycles; (h) YHN-NaM-GL.

**Table 1.** Physical Properties of YHN and Its Derived Materials

| sample | interlayer distance (Å) | $S_{BET}$ ($m^2\ g^{-1}$) |
|---|---|---|
| YHN | 8.85 | 10 |
| YHN-TA | 12.51 | |
| YHN-M | 8.12 | |
| YHN-M-EG | 8.08 | |
| YHN-NaM | | 53 |
| YHN-NaM-EG | 10.96 | 44 |
| YHN-NaM-EG* | 10.57 | |
| YHN-NaM-GL | 11.10 | |

* Recycled sample after 2 reaction runs.

YHN, YHN-M, and YHN-NaM-EG materials, the sample treated with sodium methoxide, YHN-NaM (Figure 1c), had a significant amount of amorphous structures, indicating a loss the regular crystalline phase of YHN after exposure to only 0.5 M sodium methoxide/methanol solution at 413 K for 20 h.

**3.2. XRD.** The XRD patterns of YHN and its derived materials are illustrated in Figure 2. The YHN sample displays strong layer reflections of (*00l*) at 9.99° and 19.79° as shown in Figure 2a. In addition to the strong layer reflections, a number of general (*hkl*) reflections can be observed on the YHN sample, indicating that YHN sample has excellent crystalline order.[18,22] The interlayer distances of the layered materials were calculated from XRD, and the results are reported in Table 1. The interlayer distance of the parent YHN sample was calculated to be 8.85 Å. The lanthanide hydroxides with a composition of $Ln_2(OH)_5NO_3 \cdot xH_2O$ (Ln = Y, Gd−Lu) have facile anion exchange ability with a number of inorganic and organic anions such as sulfate, carbonate, and carboxylate/dicarboxylate.[18] Consistent with the reported result, terephthalate can be easily intercalated into the interlayer space of yttrium hydroxide layered structures as shown in the XRD pattern of Figure 2b. The host layer reflections of YHN were shifted from 9.99° and 19.79° to 7.07° and 13.94°, respectively, corresponding to an interlayer spacing of 12.51 Å (Table 1) for YHN-TA. The interlayer distances of YHN and YHN-TA are slightly shorter than those previously reported by McIntyre et al.[19] at 9.18 Å and 12.8 Å, respectively. Geng et al. reported that the interlayer distance of $Ln_8(OH)_{20}(NO_3)_4 \cdot nH_2O$ (Ln = Sm, Eu, Gd, Tb, Dy, Ho, Er, Tm, and Y) materials depends on the degree of hydration.[23] The small differences were probably due to the slightly different amounts of water coordinated to the host layers between the samples of this work and those reported previously.

In addition to $Ln_2(OH)_5NO_3 \cdot xH_2O$ (Ln = Y, Gd−Lu),[18,19] $Ln_2(OH)_5X \cdot 1.5H_2O$ (X = Cl, Br; Ln = Y, Dy, Er, Yb),[20] and $RE(OH)_{2.5}Cl_{0.5} \cdot 0.8H_2O$ (RE: Eu, Tb, etc.)[21] also displayed facile anion exchange ability. However, the intercalation of alkoxide into rare-earth hydroxide layered materials has not yet been reported. Thus, the intercalation of ethylene glycol into yttrium hydroxide layered material was performed in the 0.5 M sodium methoxide/methanol solution under elevated temperature at 413 K for 20 h. The XRD pattern of YHN-NaM-EG is displayed in Figure 2f. The YHN-NaM-EG sample exhibits strong layer reflections at 8.07° and 16.11°, indicating the interlayer distance was expanded to 10.96 Å as compared to its precursor, YHN, with an interlayer distance of 8.85 Å. The overall crystallinity of the YHN-NaM-EG sample was maintained since reflections observed around 30° and 50° persisted after intercalation. Therefore, the XRD results were consistent with the observation of the similar morphology between YHN-NaM-EG and YHN as shown in Figure 1.

We speculate that ethylene glycolates ($O_2C_2H_4^{2-}$ or $O_2C_2H_5^-$) were intercalated into the interlayer space of yttrium hydroxide layered material instead of neutral ethylene glycol molecules. The formation of ethylene glycolate was accomplished by a proton transfer between methoxide anion and ethylene glycol. Without sodium methoxide, ethylene glycol could not be intercalated into yttrium hydroxide layered material. The lack of intercalation of EG in the absence of methoxide was confirmed by the XRD pattern of YHN-M-EG, as shown in Figure 2d. The interlayer distance of YHN-M-EG was 8.08 Å as shown in Table 1, which was only slightly contracted than that of YHN. The slight interlayer contraction could be due to the (partial) loss of coordinated water from YHN during the treatment of YHN with methanol and ethylene glycol at 413 K. The similarity of the XRD patterns of YHN-M (Figure 2c) and YHN-M-EG confirmed that ethylene glycol was not intercalated into the interlayer space of yttrium hydroxide layered materials in the absence of methoxide anion. Interestingly, the treatment of YHN with only sodium methoxide/methanol solution at 413 K for 20 h destroyed the crystallinity of the layered material. A totally amorphous material was formed by treatment with methoxide since no appreciable XRD reflections were observed (Figure 2e). This observation was consistent with the amorphous structures of YHN-NaM as observed by SEM.

**3.3. Fourier Transformed Infrared Spectroscopy.** The infrared spectra of YHN and its derived materials are displayed in Figure 3. The strong absorption band of YHN (Figure 3a) at 1388 $cm^{-1}$ is assigned to free nitrate anions residing in the interlayer space of yttrium hydroxide layered materials.[18,21] The YHN sample revealed a

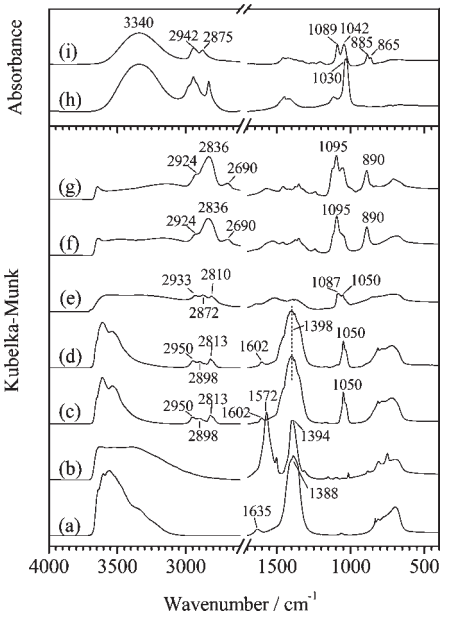


**Figure 3.** Diffuse reflectance infrared Fourier transformed spectra (DRIFTS) of solid samples: (a) YHN; (b) YHN-TA; (c) YHN-M; (d) YHN-M-EG; (e) YHN-NaM; (f) YHN-NaM-EG; (g) YHN-NaM-EG after 2 transesterification reaction cycles. Fourier transformed infrared spectra (FT-IR) of liquid samples: (h) methanol; (i) ethylene glycol.

broadband in the range of 3100−3700 $cm^{-1}$. The band between 3300 and 3700 $cm^{-1}$ is due to the H-bonded layer hydroxyl groups.[18] The shoulder at ~3350 and ~3240 $cm^{-1}$ can be ascribed to the H-bonding between nitrate anion and crystalline water similar to the features found in the layered double hydroxide materials.[33,36,37] The bending mode of the water molecule is observed at 1635 $cm^{-1}$. After the nitrate anions of YHN were exchanged by terephthalate anions, the interlayer distance was expanded to 12.51 Å, as discussed earlier. The existence of terephthalate is further confirmed by the new presence of absorption bands at 1572 and 1394 $cm^{-1}$, corresponding to the asymmetric and symmetric stretches of carboxylate anions.[18,20,33] The infrared spectra of the materials YHN-M and YHN-M-EG, displayed in Figure 3c and 3d, are almost identical to each other. Strong nitrate absorption was still present in the spectrum but was slightly shifted to ~1398 $cm^{-1}$ after treatment with methanol or methanol/ethylene glycol. The hydroxyl absorption band associated with the layers in the range of 3300−3700 $cm^{-1}$ was similar to that of YHN sample. However, the shoulders observed on YHN sample at ~3350 and ~3240 $cm^{-1}$ decreased significantly, which is likely due to the (partial) loss of coordinated water during the treatment of YHN with methanol or methanol/ethylene glycol. The water molecule bending at 1635 $cm^{-1}$ also decreased and shifted to 1602 $cm^{-1}$, probably indicating some strongly adsorbed water molecules still remained. The (partial) loss of the water from the methanol and methanol/ethylene glycol treated YHN samples is in agreement with the slightly decreased interlayer space found by XRD. Some residual adsorbed methanol molecules were observed on YHN-M and YHN-M-EG. The IR absorption bands at 2950, 2898, and 2813 $cm^{-1}$ are likely due to the C−H stretching modes of methanol. The C−O stretching band of methanol was also observed at 1050 $cm^{-1}$ on both YHN-M and YHN-M-EG samples. These features are similar to the IR spectra of liquid methanol as shown in Figure 3h. There are no obvious IR absorption features of ethylene glycol that can be observed on YHN-M-EG as compared to the IR spectra of liquid ethylene glycol as shown in Figure 3i.

The sample treated with sodium methoxide/methanol solution, YHN-NaM, had a significantly different IR spectrum to those for YHN-M and YHN-M-EG. Generally, the intensities of the absorption bands of YHN-NaM were quite weak. The nitrate band at 1388 $cm^{-1}$ was virtually eliminated on the amorphous YHN-NaM sample. Thus, methoxide likely neutralized the positively charged yttrium hydroxide layers. The presence of methoxide, probably with some physisorbed methanol molecules, can be observed by the IR absorption bands around 2750−2950 $cm^{-1}$ and 1010−1110 $cm^{-1}$. The three C−H absorption bands in YHN-M and YHN-M-EG at 2950, 2898, and 2813 $cm^{-1}$ were shifted to 2933, 2872, and 2810 $cm^{-1}$ for YHN-NaM. The C−O stretch of YHN-NaM was also shifted to 1087 $cm^{-1}$ with a small peak at 1050 $cm^{-1}$. The band shifts of the C−H stretch and the C−O stretch of YHN-NaM as compared to YHN-M/YHN-M-EG, together with the disappearance of the nitrate band, likely indicate that methoxide coordinated to the yttrium cation and neutralized the charge imbalance of the original layered material.

The IR spectra of YHN-NaM-EG in Figure 3f strongly suggest the presence of ethylene glycol or glycolate anions ($O_2C_2H_4^{2-}$ or $O_2C_2H_5^-$) in the interlayer regions. The C−H stretching bands at 2942 $cm^{-1}$ (asymmetric) and 2875 $cm^{-1}$ (symmetric) of ethylene glycol (Figure 3i) were shifted and converted into three absorption bands at 2924, 2836, and 2690 $cm^{-1}$ in YHN-NaM-EG. The absorption bands of ethylene glycol at 1089 and 1042 $cm^{-1}$ (C−O and C−C stretching) are split into several components at ~1095 $cm^{-1}$ in YHN-NaM-EG. This has also been observed in $FeO(O_2C_2H_4)_{1/2}$.[31] The two $CH_2$ rocking bands of ethylene glycol at 885 and 865 $cm^{-1}$ are merged into single band at 890 $cm^{-1}$ in YHN-NaM-EG. A similar effect has been reported in the ethylene-glycolate-substituted FeOCl layered material of $FeO(O_2C_2H_4)_{1/2}$[31] and neutral ethylene glycol intercalated into the zinc hydroxide compound of $Zn_5(OH)_8(CH_3COO)_2(HOC_2H_4OH)_2 \cdot 2H_2O$.[32] The absence of a nitrate band on YHN-NaM-EG indicated that ethylene glycolate anions, $O_2C_2H_4^{2-}$ or $O_2C_2H_5^-$, instead of neutral ethylene glycol molecules were intercalated into the yttrium hydroxide layered materials, presumably coordinated directly to the Y cations. Neutral ethylene glycol molecules have been intercalated into zinc hydroxide layered materials with acetate as charge balancing anion, in which the intense IR absorption bands of acetate at 1555 and 1440 $cm^{-1}$ were still clearly observed after intercalation.[32]

**3.4. Thermogravimetric Analysis.** The thermogravimetric analysis (TGA) of YHN is summarized in

(36) Roelofs, J. C. A. A.; van bokhoven, J. A.; van Dillen, A. J.; Geus, J. W.; de Jong, K. P. *Chem.—Eur. J.* **2002**, *8*, 5571.
(37) Hickey, L.; Kloprogge, J. T.; Frost, R. L. *J. Mater. Sci.* **2000**, *35*, 4347.

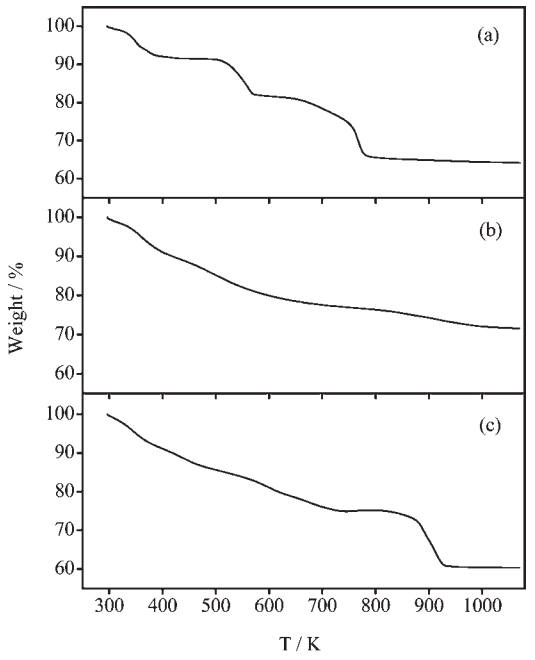


**Figure 4.** Thermogravimetric analysis of (a) YHN; (b) YHN-NaM; (c) YHN-NaM-EG.

Figure 4a. The decomposition of YHN occurs in three steps according to McIntyre et al.:[19]

$$Y_2(OH)_5NO_3 \cdot xH_2O \xrightarrow{296-450K} Y_2(OH)_5NO_3 + xH_2O \quad (4)$$

$$Y_2(OH)_5NO_3 \xrightarrow{450-615K} Y_2O_2(OH)NO_3 + 2H_2O \quad (5)$$

$$Y_2O_2(OH)NO_3 \xrightarrow{615-900K} Y_2O_3 + 0.5H_2O + NO_2 + 0.25O_2 \quad (6)$$

On the basis of the TGA results, the formula of synthesized YHN was calculated to be $Y_2(OH)_5NO_3 \cdot 1.68H_2O$. Thus, the theoretical weight ratio of $Y_2(OH)_5NO_3 \cdot 1.68H_2O/Y_2(OH)_5NO_3/Y_2O_2(OH)NO_3/Y_2O_3$ would be 1:0.915:0.814:0.636. This is in excellent agreement with the weight ratio from the YHN TGA at 296, 450, 615, and 900 K which gives 1:0.915:0.815:0.648. The amorphous YHN-NaM sample displayed a gradual weight loss upon ramping the temperature from 296 to 1073 K as shown in Figure 4b with a total weight loss of 28.3% at 1073 K. The lack of stepwise decomposition of YHN-NaM is consistent with the non-crystalline nature of the sample. In the case of YHN-NaM-EG, the ethylene glycolate intercalated sample did not fully decompose until 940 K, whereas the parent YHN sample fully decomposed below 800 K. The YHN-NaM-EG had a gradual weight loss of 25.0% up to 760 K. The weight loss below 760 K could be attributed to the removal of adsorbed methanol molecules and partial decomposition of the yttrium hydroxide layers, presumably forming $Y_2O_2(OH)(O_2C_2H_5)$ or $Y_2O_2(OH)(O_2C_2H_4)_{0.5}$, analogous to the stepwise partial decomposition of YHN between 450 and 615 K. A plateau in the thermogram of YHN-NaM-EG was observed from ~760 K to ~860 K (Figure 4c). An abrupt weight loss of 14.7% then occurred from ~860 K to ~940 K, resulting from the complete decomposition of yttrium hydroxide layers and the complete oxidation of the organic portion. The high stability of YHN-NaM-EG supports the idea that ethylene glycolate, $O_2C_2H_4^{2-}$ or $O_2C_2H_5^-$ was directly bonded to Y cations, since the normal boiling point of ethylene glycol is 470 K. A similar stabilizing effect has been reported for methoxy groups grafted in kaolinite, which decomposed at 788 K.[38] On the other hand, neutral ethylene glycol was released below 473 K from basic zinc acetate containing ethylene glycol in the interlayer regions.[32] The molecular weight ratios of $Y_2O_3$ to $Y_2O_2(OH)(O_2C_2H_5)$ and $Y_2O_3$ to $Y_2O_2(OH)(O_2C_2H_4)_{0.5}$ were 0.78 and 0.88, respectively. The former is consistent to the TGA results of the weight ratio of YHN-NaM-EG sample at 1073 to 760 K, which is 0.80. Therefore, ethylene glycolate species of $O_2C_2H_5^-$ are suggested to be intercalated into the interlayer space of yttrium hydroxide layered materials. On the basis of the TGA results on YHN-NaM-EG and assuming that methanol was the only adsorbed molecule on YHN-NaM-EG sample, the formula of YHN-NaM-EG is estimated to be $Y_2(OH)_5(O_2C_2H_5) \cdot 1.58CH_4O$. Therefore, the Y/C weight ratio will be 4.14, which is in agreement with the measured Y/C weight ratio of 4.09 by elemental analysis.

The formation of $O_2C_2H_5^-$ likely results from the transfer of a proton from ethylene glycol to methoxide as mentioned previously. During the preparation of YHN-NaM-EG, 0.5 g of YHN, which corresponded to 0.0014 mol of $Y_2(OH)_5NO_3 \cdot 1.68H_2O$, was contacted with a solution of $CH_3O^-$ (0.05 mol), $CH_3OH$ (2.4 mol), and $HOC_2H_4OH$ (0.05 mol). In the absence of the solid, the concentration of $CH_3O^-$ is estimated to be more than 1 order of magnitude greater than that of $O_2C_2H_5^-$, based on the p$K_a$ values of methanol (15.5) and ethylene glycol (15.1) at 298 K[39] and the relative high concentration of methanol. Observation of ethylene glycolate in the layered material suggests a high affinity of the solid for glycolate over methoxide.

**3.5. Transesterification.** The transesterification reaction was used to test if the sample containing ethylene glycolates could serve as a solid base catalyst. The BET surface areas of YHN and its derived materials are listed in Table 1. The YHN-NaM-EG had a surface area of 44 $m^2\ g^{-1}$, which is larger than that of YHN-NaM and less than that of YHN. Previous work in our lab showed that mobile $OH^-$ anions in the interlayer regions of hydrotalcite are effective Brønsted base catalysts for transesterification of tributyrin with methanol.[33,34] Removal of interlayer water in the hydrotalcite restricted mobility of $OH^-$ and reduced catalytic activity.[34]

The reaction profiles of reactant tributyrin (T) and product methyl butyrate (MB) are displayed Figure 5. In run 1, the YHN-NaM-EG displayed high catalytic activity. At 60 min, the tributyrin reached the conversion of 46.9% with a methyl butyrate yield of 21.9%. At 536 min, the tributyrin reached a conversion of 98.9% with a methyl butyrate yield of 93.4%. The direct recycle

(38) Tunney, J. J.; Detellier, C. *J. Mater. Chem.* **1996**, *6*, 1679.
(39) David, R. L. *CRC Handbook of Chemistry and Physics*, 90th ed.; Internet Version; CRC Press: Boca Raton, FL, 2010.

of YHN-NaM-EG revealed a significant loss in activity as shown in Figure 5. The initial activity of YHN-NaM-EG in the second run had only about 10% of the initial activity of YHN-NaM-EG in the first run. At 668 min, the tributyrin only reached conversion of 51.3% with a methyl butyrate yield of 24.2%. After two cycles of the reaction, the catalyst was separated by centrifugation and washed with 200 mL of methanol and dried with flowing $N_2$ (100 $cm^3$ $min^{-1}$) at room temperature. The XRD pattern of the recovered catalyst, YHN-NaM-EG, given in Figure 2g was similar to that of the fresh catalyst (Figure 2f) except for a slightly contracted interlayer distance of 10.57 Å. The infrared spectrum of the used YHN-NaM-EG catalyst shown in Figure 3g was almost identical to the fresh one in Figure 3f. Thus, the deactivation of YHN-NaM-EG was not due to hydrolysis side reactions, which lead to the formation of butyrate anions that can poison the catalyst. We observed in earlier work with reconstructed hydrotalcite catalysts that transesterification of tributyrin with methanol deactivated by the formation of hydrolysis side products.[33] The slightly decreased interlayer distance of the used YHN-NaM-EG could indicate leaching of the active species, which resided in the interlayer regions. To further confirm the effect of leaching, a third reaction test was performed with fresh YHN-NaM-EG. After 60 min reaction, YHN-NaM-EG was removed by filtering, and the filtrate was charged back to the reactor. Further decreases of tributyrin and increases of methyl butyrate were observed, indicating severe leaching of the active species, in agreement with the slightly decreased interlayer distance observed by the XRD. The sodium content of YHN-NaM-EG sample was measured to be 2340 ppm. Therefore, the high reactivity of fresh YHN-NaM-EG was likely due to the residual active species physisorbed on the material, probably alkoxide sodium salts. It is known that $3.14 \times 10^{-5}$ mol sodium methoxide can effectively catalyze this reaction.[33] At this point, we cannot attribute the observed initial activity to the ethylene glycolate component of the catalyst. Nevertheless, the ethylene glycolate bonded to yttrium in the layers appears to be fairly immobile because of the very low activity of the recycled catalyst.

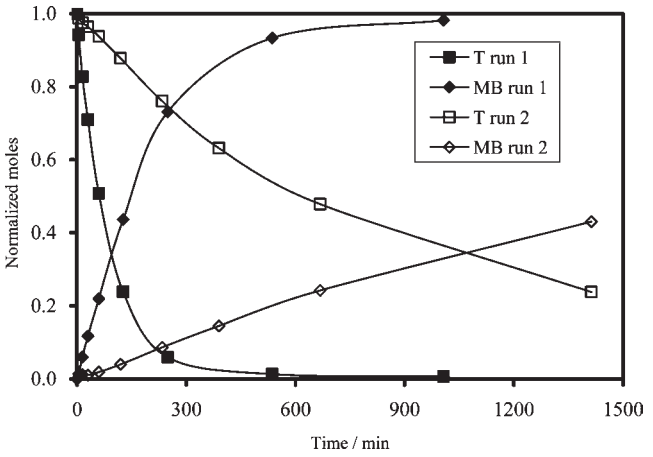


**Figure 5.** Reaction profiles of transesterification of tributyrin with methanol catalyzed by YHN-NaM-EG. The normalized moles for T and MB are defined as $y_T = [T]/[T]_0$, $y_{MB} = [MB]/[T]_0/3$, respectively, where [T] and [MB] are the concentration of T and MB (mol $L^{-1}$) and $[T]_0$ is the initial concentration of tributyrin.[33,34].

**3.6. Structure of YHN-NaM-EG.** The intercalation of ethylene glycol into YHN leads to the formation of ethylene glycolate, $O_2C_2H_4^{2-}$ or $O_2C_2H_5^{-}$, directly coordinated to a Y cation, as supported by results from XRD, FT-IR spectroscopy, TGA, and transesterification catalysis. Results from TGA and elemental analysis suggest that the bonded ethylene glycolate is likely to be $O_2C_2H_5^{-}$. The analysis of the interlayer distance of YHN-NaM-EG and the bonding between ethylene glycolate and yttrium hydroxide layer also excludes the possibility of $O_2C_2H_4^{2-}$ as charge balancing anion. If $O_2C_2H_4^{2-}$ were the charge balancing anion, two different structures could be possibly formed: one is the interlayer bridging model as shown in Scheme 2A and the other is the intralayer bridging model as shown in Scheme 2B. With the interlayer distance of YHN-NaM-EG being 10.96 Å, the interlayer bridging model is not likely to occur. The oxalate anion has similar size to $O_2C_2H_4^{2-}$; however, the oxalate anion exchanged YHN material has an interlayer distance of only 7.9 Å.[18] In addition, Kikkawa et al. estimated the interlayer distance of a model structure of the layered material of $FeO(O_2C_2H_4)_{0.5}$ with ethylene glycolate (trans configuration) bridging the adjacent layers to be 8.2 Å.[31] Kikkawa et al. then proposed that $FeO(O_2C_2H_4)_{0.5}$ has the intralayer bridging model with an interlayer distance of 10.89 Å similar to Scheme 2B that ethylene glycol coordinates to Fe ions within the same layer in a gauche configuration.[31] However, the intralayer bridging model of YHN-NaM-EG as shown in Scheme 2B is not likely to occur, since each of the $O_2C_2H_4^{2-}$ grafted yttrium hydroxide layers carries no net charge and there will be no strong attraction force between adjacent neutral layers to maintain the ordered layered structure. Indeed, the amorphous structure of the methoxide treated sample of YHN-NaM as observed by SEM and XRD provides supportive evidence that the neutralized yttrium hydroxide layers by the

**Scheme 2.** Model Structures of YHN-NaM-EG

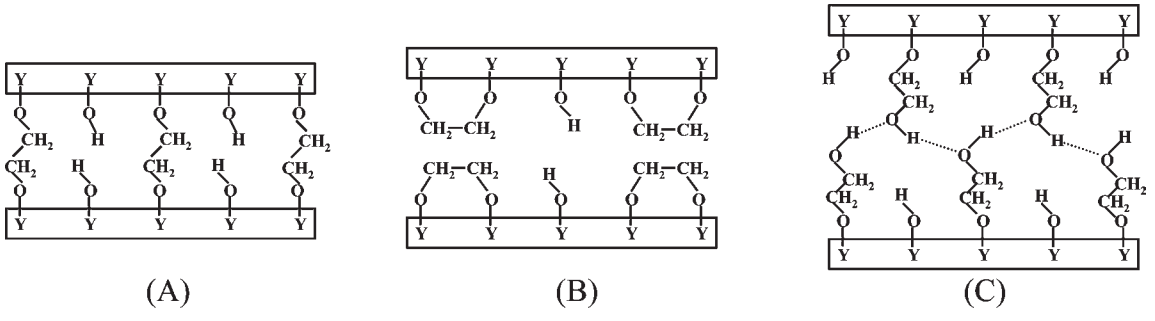

methoxide anions could not maintain a well ordered layered structure. Therefore, we can safely exclude the possibility of the intralayer bridging model of YHN-NaM-EG as shown in Scheme 2B. On the basis of above discussion, we have ruled out the formation of $O_2C_2H_4^{2-}$ as the main charge balancing anion in YHN-NaM-EG. Therefore, we suggest that $O_2C_2H_5^-$ is the anion that balances the positively charged layers of YHN-NaM-EG sample. The $O_2C_2H_5^-$ is likely bonded to the yttrium cation in the yttrium hydroxide layer. It has been observed in our control experiments involving YHN-M and YHN-M-EG that some of the coordinated water molecules can be removed by treatment of YHN with methanol or methanol/ethylene glycol. Because of the strong affinity between rare-earth elements and oxygen,[21] the treatment of YHN with 0.5 M sodium methoxide/methanol solution with ethylene glycol could lead to the replacement of a coordinated water molecule by an ethylene glycolate anion, forming a Y−O−C bond. The proposed structure of YHN-NaM-EG is presented in Scheme 2C. The well-ordered yttrium hydroxide layers grafted by $O_2C_2H_5^-$ are held together by the H-bonding between the grafted $O_2C_2H_5^-$ moieties bonded to adjacent layers. In addition to ethylene glycol, glycerol can also be intercalated into yttrium hydroxide layered materials with interlayer distance of 11.10 Å as shown in Figure 2h and Table 1. It is interesting that the interlayer distance with intercalated glycerol is only slightly greater than the material with intercalated ethylene glycol.

## 4. Conclusions

Ethylene glycol was successfully intercalated into the new layered material composed of yttrium hydroxide. It was characterized by SEM, XRD, FT-IR spectroscopy, TGA, and elemental analysis. After intercalation, the nitrate anion was replaced by ethylene glycolate ($O_2C_2H_5^-$), which was proposed to be bonded to yttrium hydroxide layers. The stacking of ethylene glycol grafted yttrium hydroxide layers is maintained by the H-bonding between the hydroxyls of grafted ethylene glycols bonded to adjacent layers. Glycerol can also be intercalated into yttrium hydroxide layered materials under similar conditions. When methoxide bonds to the yttrium cations, there is no opportunity for H-bonding to maintain the interlayer stacking, so the material delaminates and completely loses crystallinity. The strong bonding of ethylene glycolate to the yttrium hydroxide layers restricts its mobility and thus lowers its catalytic activity for base-catalyzed transesterification.

**Acknowledgment.** This work was supported by the Chemical Sciences, Geosciences and Biosciences Division, Office of Basic Energy Sciences, Office of Science, U.S. Department of Energy, Grant DE-FG02-95ER14549.